Angle-resolved photoemission study and first-principles calculation of the electronic structure of $LaSb_2$

2003 J. Phys.: Condens. Matter 15 L511

(http://iopscience.iop.org/0953-8984/15/33/101)

INSTITUTE OF PHYSICS PUBLISHING JOURNAL OF PHYSICS: CONDENSED MATTER

J. Phys.: Condens. Matter **15** (2003) L511–L517 PII: S0953-8984(03)66067-4

LETTER TO THE EDITOR

Angle-resolved photoemission study and first-principles calculation of the electronic structure of $LaSb_2$

Alice I Acatrinei[1], D Browne[1], Y B Losovyj[2], D P Young[1], M Moldovan[1], Julia Y Chan[3], P T Sprunger[1] and Richard L Kurtz[1,4]

[1] Louisiana State University, Department of Physics and Astronomy, 202 Nicholson Hall, Baton Rouge, LA 70803, USA
[2] Center for Advanced Microstructures and Devices, LSU, Baton Rouge, LA 70806, USA
[3] Louisiana State University, Department of Chemistry, Baton Rouge, LA 70803, USA

E-mail: kurtz@phys.lsu.edu

Received 16 July 2003
Published 8 August 2003
Online at stacks.iop.org/JPhysCM/15/L511

Abstract

In this work we present valence band studies of $LaSb_2$ using angle-resolved photoelectron spectroscopy with synchrotron radiation and compare these data with band structure calculations. Valence band spectra reveal that Sb 5p states are dominant near the Fermi level and are hybridized with the La 5d states just below. The calculations show a fair agreement with the experimentally determined valence band spectra, allowing an identification of the observed features. We measured some dispersion for $k_\perp$, especially for Sb 5p states; no significant dispersion was found for $k_\parallel$.

1. Introduction

Materials that react to changes in their environment are known as smart materials. Their behaviour is determined by their response to variations in luminosity, pressure, temperature, pH, electric field or magnetic field. Magnetic-field-sensitive materials have numerous applications in industry and technology, and magnetoresistive materials have been of particular interest in recent years.

The light rare-earth diantimonides, discovered about 50 years ago, exhibit interesting physical properties [1, 2]. Their magnetoresistance at low temperatures is remarkably large, and the resistance changes linearly with magnetic field [3]. The increase in zero-field resistance with temperature shows a metallic character in these compounds.

We focus on the first member of the rare-earth diantimonides, $LaSb_2$. As it is the only non-magnetic compound, its magnetic and transport properties are not complicated by magnetic

[4] Author to whom any correspondence should be addressed.

phase transitions. $LaSb_2$ has an orthorhombic crystal structure that is highly layered, with bilayers of La–Sb separated by Sb planes. Early measurements detected superconductivity in $LaSb_2$ at a temperature of 0.4 K [4, 5]. It has metallic behaviour above this temperature, and it is a weak temperature-dependent isotropic diamagnet [3]. The zero-field resistivity increases smoothly with temperature, but it shows an anomaly at around 260 K that is more obvious when current is applied parallel to the *c*-axis.

The change in zero-field resistivity is larger for a current applied parallel to the *c*-axis than for a current applied in-plane. Low-field measurements ($H < 55$ kG) reveal an anisotropic magnetoresistance, both for in-plane and for *c*-axis applied magnetic fields. The anisotropy is very pronounced at low temperatures, but is present up to 100–150 K. The *c*-axis magnetoresistance is linear for field values larger than 5–10 kG [3].

High-field temperature-dependent resistance measurements reveal an anomaly that is believed to be induced by the magnetic field. In zero field, the resistance increases with temperature. After applying a magnetic field perpendicular to the layers and a current parallel to the layers, a peak starts forming around 12 K (for 25 kG). As the field increases, the peak shifts towards higher temperatures, reaching a maximum for a magnetic field value of 180 kG, at a temperature of 26 K [3].

In order to better understand and explain the magnetotransport properties of $LaSb_2$, a description of the underlying electronic structure is essential.

2. Experiment and sample preparation

The experiments were performed at the CAMD Synchrotron Light Source (LSU, Baton Rouge, LA) on the 3 m toroidal grating monochromator (TGM) beamline, described elsewhere [6]. The end station consisted of an ultra-high vacuum system, operating at a pressure of 1.5×10^{-10} Torr, equipped with a hemispherical analyser mounted on the lower part of the main chamber. Photon energies between 17 and 80 eV were used in these studies. The photon energy resolution was 0.1–0.15 eV and the analyser was operated with a constant pass energy of 25 eV, giving an overall energy resolution of about 0.2 eV.

The $LaSb_2$ single crystals (dimensions $10 \times 10 \times 1$ mm^3) used in the experiment were grown from high-purity La and Sb using a metallic flux method [7]. The samples form in the orthorhombic $SmSb_2$ structure shown in figure 1(a), with alternating bilayers of La and Sb, separated by rectangular sheets of Sb, stacked along the *c*-axis [1, 2]. The lattice parameters as obtained from the single-crystal x-ray data refinement are $a = 6.319$ Å, $b = 6.174$ Å, and $c = 18.57$ Å, with the orthorhombic *Cmca* spacegroup [8].

$LaSb_2$ is air-sensitive, therefore the sample preparation and characterization had to take place *in situ* to avoid contamination. In both STM and photoemission measurements, the samples were cleaved *in vacuo* and at room temperature in the side chamber using a low-profile stainless steel microtome blade to expose a fresh layer at a pressure of 1.5×10^{-10} Torr.

The Auger spectra from a cleaved surface show no signs of O or C contamination, and only the Auger peaks of La and Sb are seen. Despite the fact that the material cleaves nicely leaving mirror-like surfaces, we were unable to obtain a LEED diffraction pattern. LEED measurements showed only a diffuse background with no evidence of even diffuse spots. Usually this indicates that the material must be amorphous or polycrystalline, or that the surface order is smaller than the LEED coherence length ($\sim$100 Å). In this case, Auger shows both La and Sb at the surface, so there is no clear preferential surface segregation of one component. Currently we do not know why LEED is not evident, and this observation is even more curious in light of the x-ray diffraction and the photoemission results below, which do show evidence of long-range order.

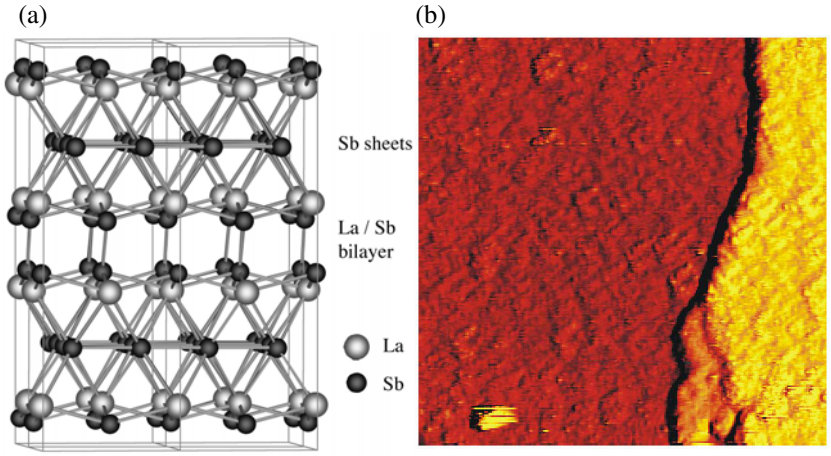

Figure 1. The orthorhombic $SmSb_2$ structure of $LaSb_2$. This shows $2 \times 2 \times 1$ unit cells with the two LaSb bilayers in the centre of the unit cell and at the unit cell c-edge. These bilayers are separated along the c-axis by rectangular sheets of Sb (La: light; Sb: dark). (b) STM image (150×150 nm^2) of $LaSb_2$ showing flat terraces separated by a step edge. The difference in height between the upper terrace (right side) and the lower terrace (left side) is ∼18 Å.

(This figure is in colour only in the electronic version)

In figure 1(b) we present a 150 nm × 150 nm STM image of $LaSb_2$ cleaved in ultra-high vacuum. The STM image shows a flat terrace through most of the image with a large step up to another flat terrace to the right. This height corresponds to a full 18.7 Å unit cell step. In the lower right of this image, one can see two step edges of approximately 9.4 Å, which is in good agreement with a half unit cell step. We were unable to obtain atomic resolution on this surface, although a quasi-periodic rumpling appeared in some images with a corrugation of ∼0.2 Å.

These data present some clues into the cleavage plane for $LaSb_2$ (001). As shown in figure 1(a), the crystal structure consists of bilayers of LaSb separated by Sb layers. Normally, materials cleave in such a manner that they present non-polar surfaces, if possible, reducing the surface free energy of the newly exposed, cleaved surfaces. This would be possible if the material were to cleave between the LaSb bilayers, resulting in two identical Sb terminated surfaces. The only other cleavage site alternative would be between a LaSb bilayer and the Sb sheet, but this would leave two different surface terminations and would probably result in patches of Sb on both. As our STM shows flat terraces without additional material, we believe that cleavage occurs between the LaSb bilayers. This can be accomplished identically at both the unit cell face and at half the unit cell height, both giving terrace separations as found in the STM measurement.

3. Photoemission results and linearized augmented-plane-wave (LAPW) density of states

We performed angle-resolved photoemission spectroscopy (ARPES) in normal emission and in angle-dependent emission geometries at two temperatures: 300 and 140 K. The lower temperature was obtained by cooling the sample stage with liquid nitrogen. We are interested in this lower temperature data since the magnetoresistance is already significant at this

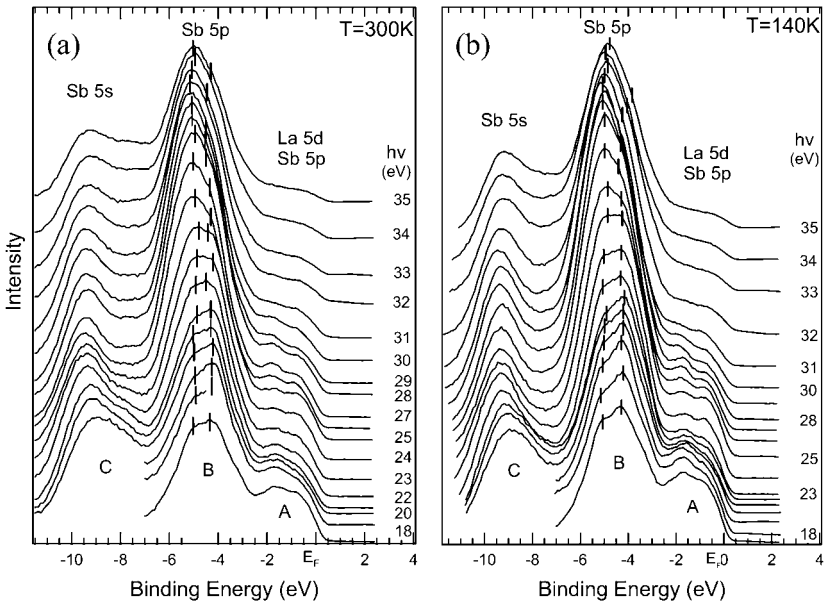

Figure 2. Normal emission spectra taken at 300 K (a) and 140 K (b) along the high-symmetry line Γ–Z. Photon energy ranged between 17 and 35 eV, with 1 eV increments.

temperature and the photoemission data may reflect underlying electronic structural changes. In these data, the photon energy was varied between 17 and 35 eV and normal-emission data were taken with 1 eV increments. Measurements were repeated on different samples from the same batch and on samples coming from different batches. All of the measurements yielded similar spectra, and confirmed the reproducibility of the data.

Figures 2(a) and (b) show the valence band photoemission spectra for $LaSb_2$ in normal emission at 300 and at 140 K. The experimental spectra reveal three distinct structures, present at both 300 and 140 K, and labelled A at about 1 eV, B located at ∼4.5 eV and C which is centred at about 9 eV. Bands A and B are each composed of two distinct features. Band A has two peaks located near 0.42 and 1.8 eV, and band B shows two features around 4.4 and 5 eV. In the case of structure C, the existence of two features, around 7.15 and 9.15 eV, is less obvious but is suggested in peak fitting calculations. All of the structures appear to be sharper at 140 K compared with measurements taken at 300 K. There is no evidence for an enhancement in the density of states (DOS) near E_F in these data as the temperature is lowered to 140 K, therefore we see no indication of charge density waves, which have been proposed as one possible mechanism for the magnetoresistance behaviour.

The angle-dependent spectra were measured for a photon energy of 30 eV, at 300 and 140 K. The electron emission angle was varied from 0° to 25° with 1° or 2° increments. Both spectra present the three structures, A, B and C, previously identified. Although the spectra look somewhat sharper at 300 K compared with 140 K, there are no regular changes in the binding energies of these peaks as a function of angle.

Additional information can be extracted by fitting these spectra as shown in figure 3(a). Our procedure involved fitting with Gaussian peaks and this reveals that at least six features are required to model the valence band spectrum. In figure 3(a) an experimental spectrum, taken at room temperature in normal emission at a photon energy of 35 eV, is indicated by the open circles. The solid curve represents the curve obtained from the sum of six Gaussian peaks,

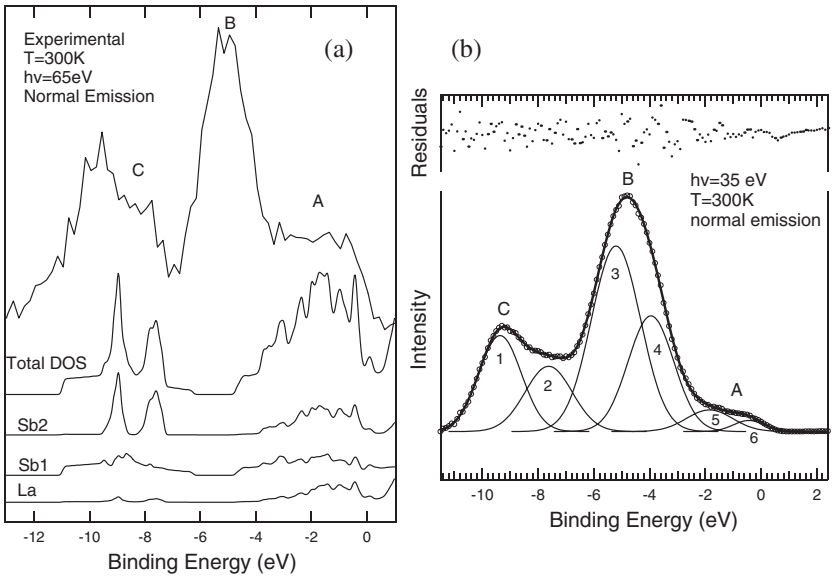

Figure 3. (a) Total DOS and partial contributions to DOS due to La and Sb, compared to an experimental spectrum taken at room temperature, for normal emission and a photon energy of 65 eV. The A, B and C structures correspond to the valence band region, while D and E indicate the core level region. (b) Experimental spectrum (empty circles) taken at room temperature, for a photon energy of 35 eV, normal emission. The solid curve represents the fitted curve obtained from the sum of six Gaussians (labelled 1 through 6).

also plotted, and the residuals to the fit are given above. We can see that our band labelled C consists of two peaks, 1 and 2, structure B is composed of peaks 3 and 4, and the valence band peak A is fit with peaks 5 and 6. The cross-section of these excitations changes with photon energy. Peaks 2 and 4 are more intense at lower photon energies while peaks 1 and 3 are more intense as the photon energy increases. Peaks 5 and 6 maintain a fairly constant intensity for all photon energies.

In order to better understand these results, we computed the electronic DOS using WIEN2K [9]. The generalized gradient approximation (GGA) for the local density was used with a grid of 1000 points ($16 \times 16 \times 3$) in the irreducible wedge of the Brillouin zone [10]. The calculations include spin–orbit interactions, which have profound effects, and local orbitals were used for both La and Sb empty states to improve the overall convergence (more details are given elsewhere [11]). The DOS was computed with a grid of 3000 points and the data were smoothed with a Gaussian of width 0.08 eV.

The total DOS is given in figure 3(b) along with the partial DOS due to La and the Sb1 (sheets) and Sb2 (bilayer) sites. These DOS are compared to an experimental spectrum plotted at the top. Those data were taken at room temperature (300 K), for normal emission and an incident photon energy of 65 eV. The shallow-core La 5p levels are seen to be spin–orbit split, between 15 and 20 eV, and the Sb 5s is found to give the peak labelled C. This latter peak also includes La admixtures of varying character, although mostly p. These levels are in reasonable agreement with the experimental data, considering that LAPW calculations do not extract core-binding energies very precisely, but there are significant differences with the bands A and B.

Band B most closely matches the Sb 5p features in the calculated DOS but there is a nearly 1 eV shift between the centroids of their spectral weights. In this case the region of

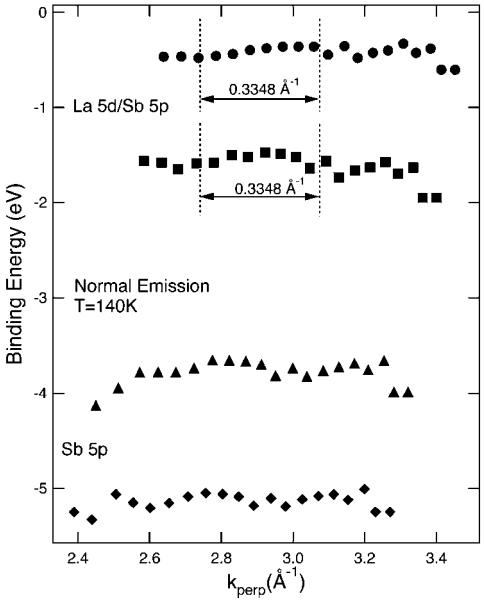

Figure 4. Experimental valence band structures along the Γ–Z symmetry line calculated for the 140 K measurements of figure 2(b).

the spectrum labelled A would correspond to a portion of the band-structure where the Sb 5p states are heavily mixed with the La 5d states. The empty La 4f states are located about 2.4 eV above E_F. A similar behaviour was determined for single-crystal LaSb: the valence bands correspond to Sb 5p states that hybridize with La 5d states [12–14]. The 4f levels are located at 2 eV above the Fermi level and hybridize strongly with the valence band [15]. A low DOS was also found for LaSb [15].

The reasons for the differences between the calculated and the measured DOS are not yet clear. For the photon energies used here, ARPES probes a thin surface layer of about 5 Å. It may be possible that due to the material's highly layered nature, the surface electronic structure differs from that of the bulk. This lack of agreement also exists for uranium intermetallics [16] and transition metal oxides, with distinct peaks outside the theoretically predicted bandwidth.

An additional feature of the band structure of $LaSb_2$ that is due to its highly layered nature, is the lack of dispersion in the direction of the 'c' axis. The theory predicts nearly all bands to be flat as one moves along the Γ to the Z direction (by changing photon energy), but there are bands located near 2 eV that are predicted to show weak dispersion of ∼0.5 eV versus $k_\perp$. We can probe this by conducting normal-emission photoemission measurements. This measures states at the $\bar{\Gamma}$ symmetry point at the surface BZ centre, and the energy dispersion is measured along the Γ to Z symmetry direction.

In figure 4 we plot the binding energies of the six features fit with the Gaussian peaks for the 140 K data of figure 2(b) after converting the data into $k_\perp$. These data are computed assuming an inner potential of 9 eV. As seen in figure 4, these data exhibit little dispersion versus $k_\perp$, consistent with the quasi-2D band structure. If we look closely at the bands nearest the Fermi surface, we see that there is some slight dispersion that is most clear for the band near 1.5 eV. For the $LaSb_2$ lattice parameters, the Brillouin zones are spaced by 0.3348 Å^{-1} along Γ to Z, and this results in the critical point Γ located at the $k_\perp$ indicated in the figure. This corresponds to an excitation to the eighth, ninth and tenth Brillouin zones for the data in figure 2.

4. Conclusion

We have performed a photoemission study of $LaSb_2$ and have identified the salient features of the data. The valence band consists largely of strongly spin–orbit split Sb 5p states, with a significant hybridization of the Sb 5p and La 5d states near the Fermi level. A prominent Sb 5s peak is found just below the valence band. We measured dispersion for $k_\perp$ from normal emission data and found that although most bands are relatively flat, dispersion can be seen for some Sb 5p states, in agreement with theory. No significant dispersion for $k_\parallel$ was found in angle-dependent measurements. Finally, no significant enhancements were observed at the Fermi level at low temperature, implying that charge density waves are not present in the region of the sample probed at the temperatures reached in this experiment.

We would like to acknowledge the support of the staff of the CAMD synchrotron light source. This work was supported in part by NSF under DMR 9802278 and ECS-0210583. One author (J Y C) would like to acknowledge NSF Career (DMR-0237664) for partial support of the project.

References

[1] Wang R and Steinfink H 1967 *Inorg. Chem.* **6** 1685
[2] Hullinger F 1979 *Handbook of Physics and Chemistry of Rare Earths* vol 4, ed K A Gschneidner and L Eyring (Amsterdam: North-Holland) p 153
[3] Bud'ko S L *et al* 1998 *Phys. Rev.* B **57** 13624
[4] Young D P, DiTusa J F, Goodrich R G, Anderson J, Guo S, Adams P, Chan J Y and Hall D 2002 *Preprint* cond-mat/0202220
[5] Hullinger F and Ott H R 1977 *J. Less-Common Met.* **55** 103
[6] Dowben P A, LaGraffe D and Onellion M 1989 *J. Phys.: Condens. Matter* **1** 6571
[7] Canfield P C and Fisk Z 1992 *Phil. Mag.* B **65** 1117
[8] Young D P, Goodrich R G, DiTusa J F, Guo S, Adams P W, Chan J Y and Hall D 2003 *Appl. Phys. Lett.* **82** 3713
[9] Hohemberg P and Kohn W 1964 *Phys. Rev.* **136** 864
[10] Blaha P, Schwarz K, Madsen G K H, Kvasnicka D and Luitz J 2001 *WIEN2k, An Augmented Plane Wave + Local Orbitals Program for Calculating Crystal Properties* ed K Schwarz (Vienna: Technical University of Vienna) ISBN 3-9501031-1-2
[11] Kurtz R L and Browne D A 2003 *Phys. Rev.* B to be submitted
[12] Kitazawa H, Suzuki T, Sera M, Oguro I, Yanase A, Hasegawa A and Kasuya T 1983 *J. Magn. Magn. Mater.* **31–34** 421
[13] Norman M R and Koelling D D 1986 *Phys. Rev.* B **33** 6730
[14] Gudat W, Iwan M, Pinchaux R and Hullinger F 1982 *Valence Instabilities* ed P Wachter and H Bopart (Amsterdam: North-Holland) p 249
[15] Olson C G, Benning P J, Schmidt M, Lynch D W and Canfield P 1996 *Phys. Rev. Lett.* **76** 4265
[16] Allen J W *et al* 1985 *Phys. Rev. Lett.* **54** 2635